Interfering single photons retreived from collective atomic excitations in two dense cold-atom clouds

Rong Cao (曹 荣), Rong Wen (温 荣), Zhenjie Gu (顾振杰), Zhiguang Han (韩枝光), Peng Qian (钱 鹏), and Jiefei Chen (陈洁菲)*

Department of Physics, East China Normal University, Shanghai 200241, China

**Corresponding author: jfchen@phy.ecnu.edu.cn*

Received March 14, 2016; accepted May 24, 2016; posted online July 6, 2016

We report the Hong–Ou–Mandel (HOM) interference, with visibility of 91%, produced from two independent single photons retrieved from collective atomic excitations in two separate cold-atom clouds with high optical depths of 90. The high visibility of the HOM dip is ascribed to the pure single photon in the Fock state that was generated from a dense-cold-atom cloud pumping by a short pulse. The visibility is always the same regardless of the time response of the single-photon detectors. This result experimentally shows that the single photons retrieved are in a separable temporal state with their idler photons.

OCIS codes: 020.4180, 190.4223, 020.3320, 270.5565.

doi: 10.3788/COL201614.080201.

The perfect destructive two-photon interference, first observed by Hong, Ou, and Mandel (HOM) with paired photons generated from spontaneous parametric down conversion (SPDC) in $\chi(2)$ non-linear crystal media[1], is one of the most well-known phenomena revealing the quantum nature of photons. HOM interference of independent single photons from separate sources is the basis of quantum swapping[2,3] and hence realistic linear optical realization of quantum repeaters[4,5]. To have complete destructive interference, each of the two independent photons must be in a pure single-photon Fock state, and they must be indistinguishable in every aspect, including polarization and spatial and spectral modes. Interfering with the single photons generated from the SPDC process in non-linear crystals has been experimentally demonstrated[6–8]. The single photons are constituted from the signal photons heralded by the correlated idler photons. In fact, two-photon interference from independent SPDC crystals is widely used in experimental demonstration of quantum swapping[9], multiphoton entanglement, etc.[10], because of the high generation rate of SPDC photon pairs.

However, SPDC schemes produce broadband photon pairs, typically with terahertz of linewidths and hence femtoseconds of coherence time. This implies a very strict synchronization between two independent SPDC processes, with which the temporal wave functions of two independent photons overlap in time at the beam splitter (BS). Passive spectral filtering can increase the coherence time, but waste a great amount of photons and thus seriously lower the generation rate. Active filtering through putting the SPDC crystal into a cavity is an efficient approach, but complicated cavity stabilization limits its further application[11,12]. With laser cooling and trapping technology developing fast, cold-atom clouds have become a new non-linear media to generate photon pairs and herald single photons. A continuous spontaneous four-wave mixing (SFWM) process in a cold-atom cloud can produce non-classical paired photons with sub-natural linewidth, determined by the transmission window caused by electromagnetically induced transparency (EIT)[13–18]. Especially with high optical depths, SFWM in an atomic ensemble can produce photon pairs with higher generation rates and longer temporal coherence[19,20]. When the pump beams in the SFWM are in the continuous mode, the atomic ensembles are always emitting photons from spontaneous Raman emission process. The paired photons and the consequent single photons are emitted randomly, with equal probability along the time axis.

In contrast, delay four-wave mixing (FWM) is composed of a “write” and a “read” process. Firstly, a pulsed pumping beam excites the atom cloud and an idler photon with a collective atomic excitation (spin wave) is written into the atom cloud. With a controllable delay time, the atomic excitation is retrieved by another pump pulse into a signal photon. The write-read scheme restricts the emission time in discrete time slots and reduces the accidental counts efficiently. A controllable single photon can be retrieved from atomic storage, and two independent and synchronized single photons are observed to produce the HOM dip and a polarization entangled state[21,22]. More importantly, the coherence time of the resulting paired photons is of the order of nanoseconds, and thus the time tolerance for synchronization is much greater than the SPDC scheme[23,24]. Therefore, the write-read scheme in an atomic ensemble is a more accessible approach to producing indistinguishable single photons between independent sources. Different from continuous FWM, the paired photons generated in this write-read scheme do not have time-frequency entanglement[25]. The temporal function of the paired photons can be factorized as the product of temporal function of two individual photons[26]. Hence, the single photons heralded are in a separable temporal state with their trigger photons.

In this Letter, through interfering single photons from the write-read scheme, i.e., from retrieving an atomic excitation written from two independent dense cold atomic clouds, we demonstrate the purity and indistinguishability of the single photons. By utilizing a dense cold atomic ensemble with a high optical depth (OD = 90), we maintain a high excitation rate in the write process. With the full width at half-maximum of a pump pulse as 100 ns and a maximum power of 100 μW, the excitation probability, which is defined as the generation probability of the idler photons in the first Raman process, is 2.3×10^{-3}. After a strong read optical beam, an anti-Stokes photon is retrieved. Concerning the Stokes and anti-Stokes paired photons, the normalized second-order cross correlation reaches 571, violating the Cauchy–Schwartz inequality by a factor of 8.1×10^4 and indicating a strong non-classical correlation. The purity and indistinguishability of the heralded single photons are tested via HOM interference between single photons from two separate and independent cold-atom clouds. The fitted visibility is as high as 91%, and the width of the HOM dip is about 99 ns, which agrees with the coherence time of the photon pairs. Finally, we report that the visibility of HOM interference is not dependent on the response time of the single-photon detectors. This is experimental proof of the fact that the temporal state of the paired photons from the delay FWM process is separable.

Figure 1(a) shows the energy level scheme for the delay FWM process in each MOT, in which $|1\rangle = 5S_{1/2}$, $F = 2$; $|2\rangle = 5S_{1/2}$, $F = 3$; $|3\rangle = 5P_{1/2}$, $F = 3$, and $|4\rangle = 5P_{3/2}$, $F = 3$. The write beam pumps the first spontaneous Raman transition, with frequency detuning $\Delta\omega_p = 146$ MHz and a center wavelength of 780 nm. The read beam is working on resonance with the transition $|2\rangle \rightarrow |3\rangle$, with a center wavelength of 795 nm. The atoms are initially pumped to the hyperfine atomic level $|1\rangle$, which is easily achieved by controlling the timing of the laser cooling process. Figure 1(b) shows the timing scheme of the experiment. In the first part of the cycle with 4.5 ms, we prepare the cold-atom cloud in a two-dimensional magneto-optical trap (MOT). The repump beam is turned off 0.3 ms earlier than the cooling beam to optically pump all the atoms onto $|1\rangle$. The optical depths of both MOTs are about 90[27]. After that, all the cooling and repump beams are turned off, and a 0.5 ms of photon pair generation window starts. In this window, the pump and read pulses sequentially repeat with multiple shoots $N = 700$ to generate Stokes photons and retrieve anti-Stokes photons from collective atomic excitations. The timing schemes in both MOTs are the same, but with the time difference Δt between them tunable. In each MOT, the write (σ^+ polarized) and read beams (σ^- polarized) are applied onto the atom cloud, with an angle separation of 3° with respect to the longitudinal axis of the cloud, which is also the collection axis of the photon pairs. We use a pair of quarter-wave plates and a polarization beam splitter (PBS) to collect the circularly polarized Stokes (σ^+) and anti-Stokes (σ^-) fields. The photons are directed into two input ports

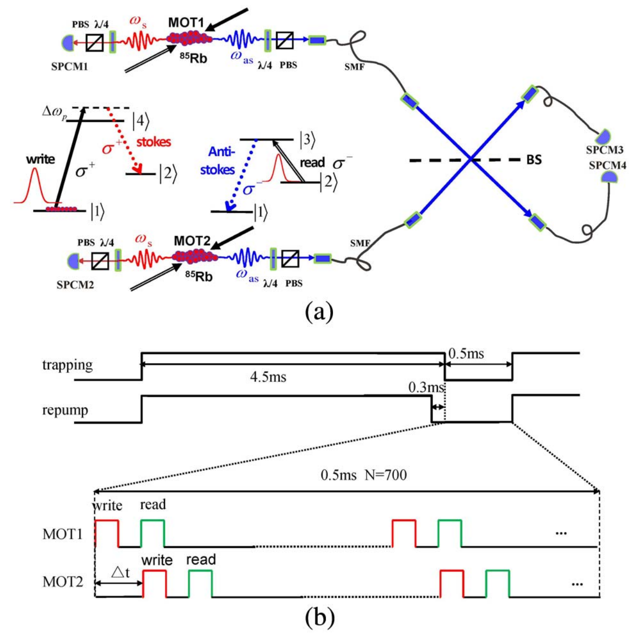

Fig. 1. (a) SFWM experimental setup. The ^{85}Rb atomic ensemble is prepared in a two-dimensional MOT. Energy level for photon pairs in ^{85}Rb atomic ensemble. $|1\rangle = |5S_{1/2}, F = 2\rangle$, $|2\rangle = |5S_{1/2}, F = 3\rangle$, $|3\rangle = |5P_{1/2}, F = 3\rangle$, $|4\rangle = |5P_{3/2}, F = 3\rangle$. HOM interferometer: single photons from MOT1 and MOT2 mix at a 50:50 BS. We use four SPCMs to detect the photons. (b) Timing control for write and read lasers in MOT1 and MOT2. For each MOT, the write and read lasers are separated by an identical delay time and the total experiment time consists of N write-read cycles. In our experiment, we use the Δt between the starting edge of the pump pulses of MOT1 and MOT2 to separate the temporal waveforms of the independent single photons.

of a 50/50 BS and collected again at two output ports with single-photon counting module SPCMs. Therefore, if both SPCM1 and SPCM2 click, each atom cloud is successfully written into atomic excitation. The retrieved single photons interfere, and they are collected by SPCM3 and SPCM4.

We apply a sequence of write and read pulses onto each MOT to generate Stokes and anti-Stokes paired photons, as shown in Fig. 1(b). Every short pump and read pulse can be represented by a Gaussian function e^{-2t^2/σ^2}, with $\sigma = 50$ ns. The maximum Rabi frequencies of the write and read beams are $2\pi \times 3.4$ and $2\pi \times 29.2$ MHz, respectively. The weak and far-detuned write pulses excite the atom cloud and produce a Stokes photon along with an atomic excitation written into the atomic ensemble. The atomic excitation can be stored for about 1 μs, which is determined mainly by the decoherence caused by the residual magnetic field. To maximize the retrieval efficiency, we apply a strong read pulse of 60 ns (delay time τ_d) after the pump pulse. The read beam is on resonance, and therefore, the anti-Stokes photons are retrieved from the atomic excitation with the assistance of the EIT effect. Since the read beam creates a very strong coupling field at the transition $|2\rangle \rightarrow |3\rangle$, the group delay of the

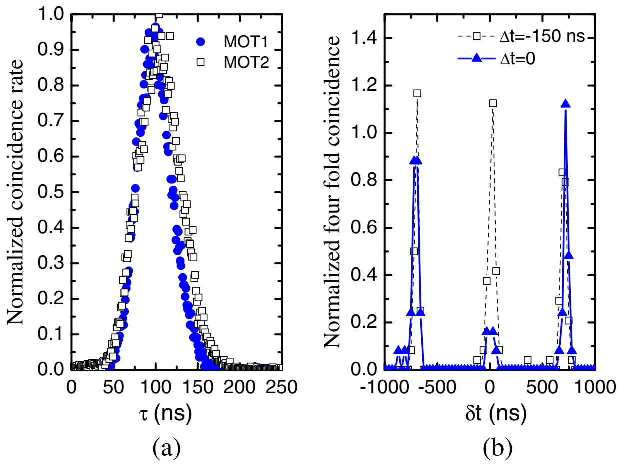

Fig. 2. (a) Normalized coincidence rates of MOT1 and MOT2, $\tau = t_{\mathrm{as}} - t_s$ is the relative time delay of the anti-Stokes photons. (b) Fourfold coincidence as a function of δt, the time difference between the arrival of the Stokes photons. The experimental data show two cases: $\Delta t = 0$ ns (blue triangles) and $\Delta t = -150$ ns (dark squares). A time step of δt axis is 30 ns.

anti-Stokes photons is minimized and does not influence the correlation function of the paired photons. The temporal coherence of the paired photons is determined by the width of the write pulse. The normalized coincidence rate of the paired photons is shown in Fig. 2(a), resembling the Gaussian function of the write beam. With the parameters described above, the excitation probability of a Stokes photon from a pump pulse is $P_S = 2.3 \times 10^{-3}$. The retrieval efficiency of the anti-Stokes photons from collective atomic excitations is measured to be 7%. After considering 50% for the quantum efficiency of each SPCM, 80% for each Fabry–Perot filter, and 63% for the mode matching between the Stokes and anti-Stokes fields, we obtain a retrieval efficiency after loss correction as high as 70%.

To indicate the non-classical property of the generated paired photons and the single photon heralded, we calculate the second-order cross correlation for the paired photons. The normalized second-order cross-correlation function is

$$g^{(2)}_{s,\mathrm{as}}(\tau) = G^{(2)}_{s,\mathrm{as}}(\tau)/R_s R_{\mathrm{as}} \Delta\tau T, \tag{1}$$

in which $\Delta\tau$ is the time resolution of the coincidence measurement, and T is the measurement time. According to the coincidence results shown in Fig. 2(a), $g^{(2)}_{s,\mathrm{as}}$ can reach a maximum value of 571. Therefore, the Cauchy–Schwartz inequality[28] between the Stokes and anti-Stokes fields is violated by a factor of $R = 8.1 \times 10^4$, much higher than the result obtained in the same excitation probability P_S given in Ref. [26]. On the other hand, we measure the second-order autocorrelation function $g^{(2)}_c = 0.07 \pm 0.01$ of the anti-Stokes photons, heralded by the paired Stokes photons. An ideal single photon in the Fock state gives $g^{(2)}_c = 0$, while $g^{(2)}_c < 0.5$ gives an upper bound.

Figure 2(b) shows the normalized fourfold coincidence counts with respect to the time delay δt between two Stokes photons from independent MOTs. Two different cases, $\Delta t = 0$ and $\Delta t = -150$ ns, are shown Fig. 2(b). For $\Delta t = 0$, when the time delay between the trigger photons is zero, two single photons coincide at the BS and will exit through a same output port due to their Bosonic nature. Therefore, the blue triangles in Fig. 2(b) show a dramatic reduced fourfold coincidence rate at $\delta t = 0$, i.e., when the temporal waveforms of two independent single photons totally overlap. The visibility is obtained as $V = 1 - R_{\min}/\bar{R}_{\max} = 0.84$, in which the maximum coincidence rate $\bar{R}_{\max}$ is obtained from averaging the rates of adjacent peaks, which shows the coincidence when no photon interference occurs. When two single photons do not coincide at the BS, i.e., $\Delta t = -150$ ns, the two-photon interference does not occur. The dark empty squares in Fig. 2(b) indicate that the normalized coincidence rate is 1 at zero time delay. If we vary Δt, the fourfold coincidence counts at zero time delay change according to the overlap of the temporal correlation function of two single photons at the BS. Therefore, the HOM interference dip is obtained through varying the time difference Δt between the write-read sequences of two independent MOTs.

Figure 3 shows the fourfold coincidence rates when summarizing the counts in the center peak in Fig. 2(b), as a function of Δt. The vertical axis shows the normalized coincidence probability, which is 1 at the wings of the HOM interference curve. The dark dots with error bar indicate the experimental data, and the red solid line shows its Gaussian fit $1 - e^{-2t^2/\sigma_f^2}$, with $\sigma_f = 99$ ns. This temporal width of the HOM interference curve agrees with the second-order correlation function of the photon pairs from each MOT in Fig. 2(a). As we have pointed out, the width of the write pulse determines the temporal width of the correlation function, and hence it controls the width of the HOM dip. In our experiment, the misalignment of the write-read timing sequences of two MOTs can be

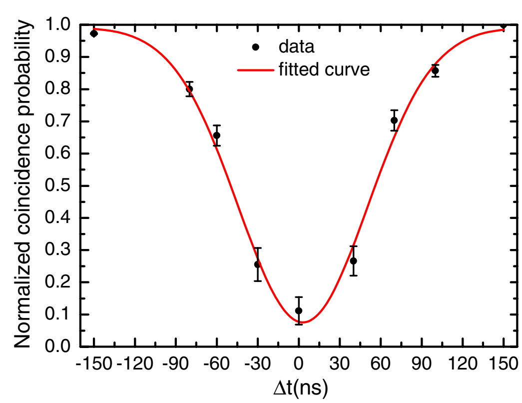

Fig. 3. Normalized coincidence probability as a function of Δt. The accidental coincidence is also shown in the figure. The whole figure expresses the "HOM DIP." The solid line is the Gaussian fit for normalized coincidence probability. From the fitted line, we get the visibility in the experiment = 0.91.

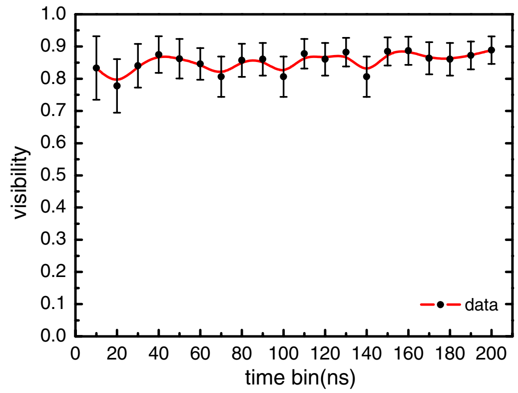

Fig. 4. Visibility versus time bin. The visibility is consistent, with error bars shown. The HOM dip can be measured by any single-photon counting module.

tolerated up to ±50 ns. The visibility of the HOM dip obtained from this fitting is 0.91, indicating a good purity and indistinguishability of independent single photons from two identical cold-atom clouds. Different from SPDC in non-linear crystals, the write-read scheme in cold atomic ensembles generates narrow-band photon pairs and single photons, which make it easier to synchronize independent quantum sources separated from a large distance.

Different from the time-frequency entangled photon pairs produced by continuous FWM, the Stokes and anti-Stokes photons produced from the delay FWM scheme do not have frequency correlation. If we represent the two-photon state of the paired photons as

$$|\Psi\rangle = \int d\omega_s d\omega_{\mathrm{as}} \Phi(\omega_s, \omega_{\mathrm{as}}) \hat{a}_s^\dagger(\omega_s) \hat{a}_{\mathrm{as}}^\dagger(\omega_{\mathrm{as}}) |0\rangle_s |0\rangle_{\mathrm{as}}, \quad (2)$$

when the joint amplitude can be factorized as $\Phi(\omega_s, \omega_{\mathrm{as}}) = \varphi(\omega_s)\phi(\omega_{\mathrm{as}})$, the spectral state of the photon pair is separable[29]. The heralded anti-Stokes photon is hence pure in the time-frequency domain, regardless of the time response of the detectors that measure the arrival time of the triggering Stokes photons. Figure 4 shows the visibility $V = 1 - R_{\min}/R_{\max}$ of the HOM dip as a function of the time bin of the time delay axis δt in Fig. 2(b). In this plot, we change the time bin from 10 to 200 ns, which is sufficiently larger than the coherence time of the photon pairs. The visibility maintains a consistent value, i.e., 0.85 ± 0.07, with different time bins. Despite the slowness of the single-photon detectors, photon pairs with factorable joint amplitudes produce pure heralded single photons. The fact that the paired photons emitted from the delay FWM are not time-frequency entangled can be explained as follows: the single photons are retrieved when we apply a strong read field onto the atom cloud, and therefore the generation time of the single photon is controllable.

In conclusion, we generate single photons retrieved from atomic excitation written into a cold-atom cloud via spontaneous Raman transition. In the write-read process, non-classical paired photons are emitted from the cold-atom cloud. With high optical depth, the atomic ensembles produce Stokes photons with an excitation probability of 2.3×10^{-3}, while the normalized second-order cross correlation of the photon pairs reaches 571. The heralded single photons are pure and indistinguishable, and we have observed an HOM dip with a visibility of 91% when interfering two independent single photons from separate cold-atom clouds. Also, we demonstrate that the visibility of the HOM dip is maintained even when the single photon detectors are ultra slow and not able to resolve the temporal correlation function. This is an experimental proof of the factorable joint amplitude for the non-classical photon pairs.

This work was supported by National 973 Program of China (No. 2011CB921604), the National Natural Science Foundation of China (NSFC) through the major research plan (Precision Measurement Physics Grant No. 91436211), the NSFC Key Research Program (No. 11234003), and the Young Scientists Research Program (No. 11204086).

References

1. C. K. Hong, Z. Y. Ou, and L. Mandel, Phys. Rev. Lett. **59**, 2044 (1987).
2. J. W. Pan, D. Bouwmeester, H. Weinfurter, and A. Zeilinger, Phys. Rev. Lett. **80**, 3891 (1998).
3. H. de Riedmatten, I. Marcikic, J. A. W. van Houwelingen, W. Tittel, H. Zbinden, and N. Gisin, Phys. Rev. A **71**, 050302 (2005).
4. Z. S. Yuan, Y. A. Chen, B. Zhao, S. Chen, J. Schmiedmayer, and J. W. Pan, Nature **454**, 1098 (2008).
5. S. Chen, Y. A. Chen, B. Zhao, Z. S. Yuan, J. Schmiedmayer, and J. W. Pan, Phys. Rev. Lett. **99**, 180505 (2007).
6. T. Legero, T. Wilk, M. Hennrich, G. Rempe, and A. Kuhn, Phys. Rev. Lett. **93**, 070503 (2004).
7. R. Kaltenbaek, B. Blauensteiner, M. Żukowski, M. Aspelmeyer, and A. Zeilinger, Phys. Rev. Lett. **96**, 240502 (2006).
8. T. Yang, Q. Zhang, T. Y. Chen, S. Lu, J. Yin, J. W. Pan, Z. Y. Wei, J. R. Tian, and J. Zhang, Phys. Rev. Lett. **96**, 110501 (2006).
9. R. Kaltenbaek, R. Prevedel, M. Aspelmeyer, and A. Zeilinger, Phys. Rev. A **79**, 040302 (2009).
10. J. W. Pan, Z. B. Chen, C. Y. Lu, H. Weinfurter, A. Zeilinger, and M. Żukowski, Rev. Mod. Phys. **84**, 777 (2012).
11. M. Halder, A. Beveratos, R. T. Thew, C. Jorel, H. Zbinden, and N. Gisin, New. J. Phys. **10**, 023027 (2008).
12. J. Yang, X. H. Bao, H. Zhang, S. Chen, C. Z. Peng, Z. B. Chen, and J. W. Pan, Phys. Rev. A **80**, 042321 (2009).
13. S. Du, P. Kolchin, C. Belthangady, G. Y. Yin, and S. E. Harris, Phys. Rev. Lett. **100**, 183603 (2008).
14. S. Du, C. Belthangady, P. Kolchin, G. Y. Yin, and S. E. Harris, Opt. Lett. **33**, 2149 (2008).
15. D. Wei, J. F. Chen, M. M. T. Loy, G. K. L. Wong, and S. Du, Phys. Rev. Lett. **103**, 093602 (2009).
16. Z. Bai, C. Hang, and G. Huang, Chin. Opt. Lett. **11**, 012701 (2013).
17. Y. Ma, J. Deng, Z. Hu, H. He, and Y. Wang, Chin. Opt. Lett. **11**, 022701 (2013).
18. H. Chen, K. Ying, Y. Duan, Y. Niu, and S. Gong, Chin. Opt. Lett. **12**, 092701 (2014).
19. L. W. Zhao, X. X. Guo, C. Liu, Y. Sun, M. M. T. Loy, and S. Du, Optica **1**, 84 (2014).

20. Z. Han, P. Qian, L. Zhou, J. F. Chen, and W. P. Zhang, Sci. Rep. **5**, 9126 (2015).
21. J. Hofmann, M. Krug, N. Ortegel, L. Gérard, M. Weber, M. Weber, and H. Weinfurter, Science **337**, 72 (2012).
22. Z. S. Yuan, Y. A. Chen, S. Chen, B. Zhao, M. Koch, T. Strassel, Y. Zhao, G. J. Zhu, J. Schmiedmayer, and J. W. Pan, Phys. Rev. Lett. **98**, 180503 (2007).
23. V. Leong, S. Kosen, B. Srivathsan, G. K. Gulati, A. Ceré, and C. Kurtsiefer, Phys. Rev. A **91**, 063829 (2015).
24. C. Liu, J. F. Chen, S. Zhang, S. Zhou, Y. H. Kim, M. M. T. Loy, G. K. L. Wong, and S. Du, Phys. Rev. A **85**, 021803(R) (2012).
25. S. Du, Phys. Rev. A **92**, 043836 (2015).
26. P. J. Mosley, J. S. Lundeen, B. J. Smith, P. Wasylczyk, A. B. U'Ren, C. Silberhorn, and I. A. Walmsle, Phys. Rev. Lett. **100**, 133601 (2008).
27. J. Zhang, Z. Gu, P. Qian, Z. Han, and J. F. Chen, Chin. Phys. Lett. **32**, 064211 (2015).
28. M. D. Reid and D. F. Walls, Phys. Rev. A **34**, 1260 (1986).
29. S. Chen, Y. A. Chen, T. Strassel, Z. S. Yuan, B. Zhao, J. Schmiedmayer, and J. W. Pan, Phys. Rev. Lett. **97**, 173004 (2006).